Available online at www.sciencedirect.com
SCIENCE DIRECT
Journal of Power Sources 155 (2006) 461–469
JOURNAL OF POWER SOURCES
www.elsevier.com/locate/jpowsour

The effect of additives on the electrochemical properties of Fe/C composite for Fe/air battery anode

Bui Thi Hang [a,*], Tomonori Watanabe [a], Minato Egashira [b,1], Izumi Watanabe [b], Shigeto Okada [b], Jun-ichi Yamaki [b]

[a] *Interdisciplinary Graduate School of Engineering Sciences, Kyushu University, 6-1 Kasuga-koen, Fukuoka 816-8580, Japan*
[b] *Institute for Materials Chemistry and Engineering, Kyushu University, 6-1 Kasuga-koen, Fukuoka 816-8580, Japan*

Received 4 April 2005; received in revised form 16 April 2005; accepted 16 April 2005
Available online 29 June 2005

Abstract

K_2S and FeS were employed as additives for electrolyte and electrode, respectively, to suppress hydrogen evolution and improve the cycleability of the Fe/C composite air battery anode. The effects of these additives on the electrochemical properties of Fe/C composite electrodes were investigated using cyclic voltammetry (CV). The results showed that both K_2S and FeS significantly suppressed hydrogen evolution on the Fe/C electrode characteristics. Among the carbons used, nano-carbons such as tubular carbon nanofibers (CNF), platelet CNF, vapor-grown carbon fibers (VGCF) and acetylene black (AB) improved the discharge capacity of the Fe/C electrode with additive to electrolyte or electrode. The FeS additive showed a larger beneficial effect for the Fe/C composite electrode than K_2S in term of cycleability and capacity.

Keywords: Nano-carbon; Additive; Iron/carbon nanocomposite; Iron–air battery anode

1. Introduction

Developmental studies on porous iron electrodes have received attention in recent years because of their use in Ni–Fe and Fe–air cells [1–4,16,19–23,29–30]. However, the major problem of iron electrode is its passivation caused by iron hydroxide produced during the discharge process, preventing further anodic utilization. Furthermore, the porous iron electrode has a low hydrogen overpotential, which limits its application in commercial batteries [1,15,18,21,23]. Hydrogen evolution competes with $Fe(OH)_2$ reduction during the charge process, which makes overcharge necessary and give rise to poor charge efficiency [6,23]. In addition, the hydrogen evolution occurring at open circuit causes the corrosion of the iron electrode and results in a high self-discharge rate [23]. Therefore, numerous investigations have focused on improving charging efficiency, discharge capacity and minimizing self-discharge [5–31].

Although various metal sulphides have been employed as additives with iron electrodes and associated electrolyte in order to circumventing these problems, its role is not yet fully understood. The effectiveness of the sulfide additive has been attributed to factors such as sulphide ion adsorption at the electrode/electrolyte interface with subsequent incorporation into the oxide lattice [5,6,10], modification of electrode kinetics [5], modification of the electrode texture and morphology [10], increase in the anodic current density [10,13,22], increase in the bulk electrode conductivity [15], enhancing the rate of the $Fe/Fe(OH)_2$ reaction, increase in the solubility of iron compounds [10,12,21–22], and inhibition the self-discharge of the iron electrode [6,7,23]. Studies showed that the addition of both FeS (or sulphur)

* Corresponding author. Tel.: +81 92 583 7841; fax: +81 92 583 7790.
E-mail addresses: hang@cm.kyushu-u.ac.jp, hanglong812@yahoo.com (B.T. Hang).
[1] Present address: Faculty of Engineering, Yamaguchi University 2-16-1, Tokiwadai, Ube, Yamaguchi 755-8611, Japan.

0378-7753/$ – see front matter © 2005 Elsevier B.V. All rights reserved.
doi:10.1016/j.jpowsour.2005.04.010

to the electrode active material [3,7,10–13,15–18,20,22,23] and Na_2S (or K_2S) to the KOH electrolytic solution [3,5–9,12–14,19,21] increases significantly the iron electrode capacity. Beside that, LiOH was used as additive to KOH electrolyte [5,7,12,14] to improve the utilization of iron electrode. However, most of the studies have mainly been conducted with an iron wire, planar, a sintered iron electrode [5–12,14–20,22–31] or an iron oxide electrode [13,21] by employing fast sweep techniques, which exhibit non-equilibrium behavior. Our previous work [32] revealed that Fe/C mixed electrode improves the conductivity and redox current. In the present study, the effects of K_2S and FeS additives on the Fe/C mixed electrode were investigated.

2. Experimental

Vapor-grown carbon fibers (VGCF; Showa Denko Co.), acetylene black (AB, Denki Kagaku Co.) and natural graphite (Chuetsu Graphite Co.), with average diameters of ca. 200 nm, 100 nm and 18 μm, respectively, were used in the present work. In addition, two kinds of carbon nanofibers (CNFs), of the nanotube type, having an average diameter of ca. 50 nm, and a platelet type, having an average diameter of ca. 150 nm, were also investigated. For tubular CNF, hexagonal planes compose hollow tubes, while in platelet CNF, a smaller hexagonal plane is stacked perpendicular to the fiber axis. Iron powder (Wako Pure Chemical, Co.) was used for an iron source. The main characteristics of the carbon materials employed and iron powder were listed in Table 1 and their morphology was shown in Fig. 1.

In order to obtain the electrochemical behavior of each Fe/C material, two types of electrode, with and without FeS additive, were prepared. The electrode sheet free additive was prepared by mixing of 45 wt.% the respective carbon, 45 wt.% iron powder and 10 wt.% polytetrafluoroethylene (PTFE; Daikin Co.) and rolling. Fe/C composite electrodes containing FeS additive were prepared by the same procedure. FeS, which was present at three levels 0.5 wt.%, 1 wt.% and 2 wt.% in the FeC electrode, was incorporated into the Fe/C electrodes by mixing before rolling. The Fe/C composite electrode was made into a pellet of 1 cm diameter. Two kinds of electrolyte were prepared, without additive (base electrolyte) and with additive. The based electrolyte was 8 mol dm^{-3} aqueous KOH solution and the additive electrolyte was KOH solution containing 0.01, 0.05 and 0.1 M of K_2S or 0.5 M LiOH (total concentration of KOH and K_2S or LiOH is 8 M). Cyclic voltammetry studies were carried out with a three-electrode glass cell assembly that had the Fe/C electrode as the working electrode, silver oxide as the counter electrode, Hg/HgO (1 M NaOH) as the reference electrode and cellophane, together with filter paper, as the separator, which was sandwiched by the two electrodes. The based electrolyte was used for electrode with FeS additive and the electrolyte containing K_2S or LiOH was applied for sulfide free electrode. Cyclic voltammetry measurements were recorded at a sweep rate of 0.5 mV s^{-1} and in the range of −1.2 to −0.1 V.

Table 1
Main characteristics of the carbon materials and iron powder

	Grain size (nm)	BET surface area ($m^2\ g^{-1}$)	True density ($g\ cm^{-3}$)
VGCF	100–300	13	2.21
AB	40–100	68	2.0
Natural graphite	18000	8	2.24
Tubular CNF	20–100	92	2.09
Platelet CNF	40–200	91	2.10
Iron	<4500	–	–

3. Results and discussion

3.1. Effect of K_2S additive

The voltammograms of the Fe/C electrode in base electrolyte and in electrolyte containing 0.1 M of the K_2S additive after five initial cycles are shown in Fig. 2. From these profiles it is clear that the carbon component and K_2S additive strongly affect the redox behavior of iron. In the case of Fe/C electrode in electrolyte without K_2S additive (Fig. 2a), the two oxidation peaks were observed around −0.85 V (a_1) and −0.65 V (a_2), respectively while a single reduction peak occurred around −1.0 V (c_1). The previous investigation [12] indicated that the clear surface of iron was never exposed to the electrolyte, and over a partially oxidized surface, adsorption of hydroxyl ion takes place. The dissolution of the oxide or underlying metal by the ion transport through the oxide can also take place. The overall electrochemical behavior involved in the passivation and dissolution of iron in alkaline solution was proposed earlier [1,2,12–15,24,25,27–31] containing two main steps, the first of which: Eq. (1) of [1]

$$Fe + 2OH^- \rightleftarrows Fe(OH)_2 + 2e, \quad E^0 = -0.975\ V \tag{1}$$

According to some authors [12,14,24,25], Eq. (1) involves the following partial steps in conjunction with the adsorption of OH^- ion:

$$Fe + OH^- \rightleftarrows [Fe(OH)]_{ad} + e \tag{2}$$

$$[Fe(OH)]_{ad} + OH^- \rightleftarrows Fe(OH)_2 + e \tag{3}$$

Most authors agree that the formation of $Fe(OH)_2$ proceeds through the formation of intermediate soluble species $HFeO_2^-$ [1,2,14,19,27–31], whose concentration is strongly temperature dependent [12,24,25], i.e.:

$$[Fe(OH)_{ad} + 2OH^- \rightleftarrows HFeO_2^- + H_2O + e \tag{4}$$

and

$$HFeO_2^- + H_2O \rightleftarrows Fe(OH)_2 + OH^- \tag{5}$$

The second oxidation step of iron electrode involves: Eq. (6) of [1]

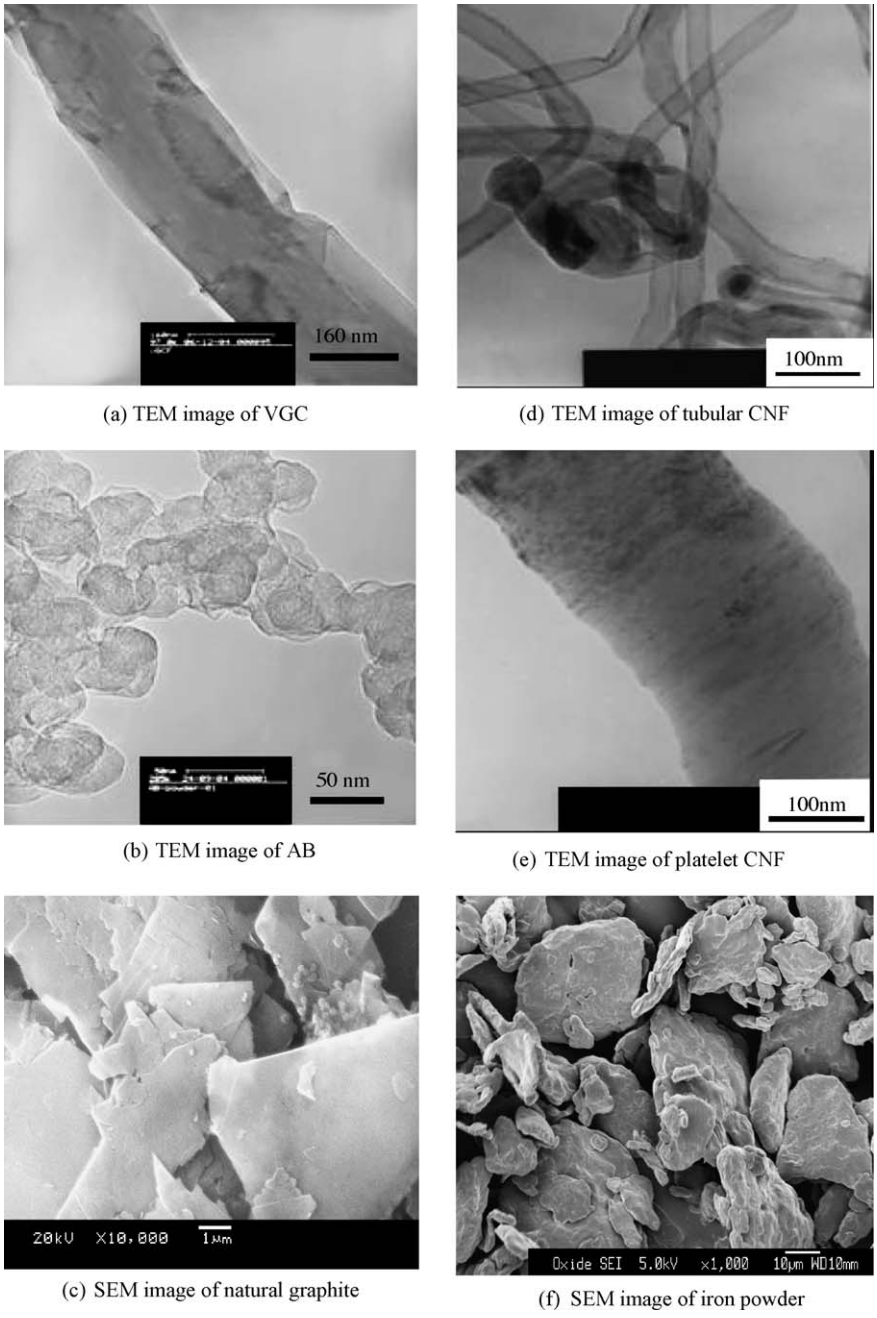

(a) TEM image of VGC
(d) TEM image of tubular CNF
(b) TEM image of AB
(e) TEM image of platelet CNF
(c) SEM image of natural graphite
(f) SEM image of iron powder

Fig. 1. Morphology of carbon materials and iron powder.

$$Fe(OH)_2 + OH^- \rightleftarrows FeOOH + H_2O + e, \quad E^0 = -0.658\,V \tag{6}$$

and/or Eq. (7) of [13,14]

$$3Fe(OH)_2 + 2OH^- \rightleftarrows Fe_3O_4{\cdot}4H_2O + 2e, \quad E^0 = -0.758\,V \tag{7}$$

The effect of the carbon component on the redox behavior of Fe/C electrode was clearly presented from CV profiles. For example, in the case of without K_2S additive (Fig. 2a), tubular CNF, platelet CNF and acetylene black provided a sharp reduction peak around −1.0 V (c_1) and a corresponding oxidation peak around −0.65 V (a_2), with a small oxidation peak around −0.85 V (a_1). The first anodic peak (a_1) is attributed to oxidation of Fe to Fe(II) (Eq. (1)). Since anodic charge corresponding to peak (a_1) is considerably smaller than that corresponding to the peak (a_2) therefore the second anodic peak (a_2) involves oxidation of both Fe to Fe(II) (Eq. (1)) and Fe(II) to Fe(III). During the first scan, the Fe(II) was converted to Fe(III) as shown in Eqs. (6) and (7), however, from the second scan, the oxidation of Fe(II) was proceeded only through Eq. (7) as evidenced by the Fe_3O_4 production including Fe(II) and Fe(III). Thus, the cathodic peak (c_1) corresponds to the

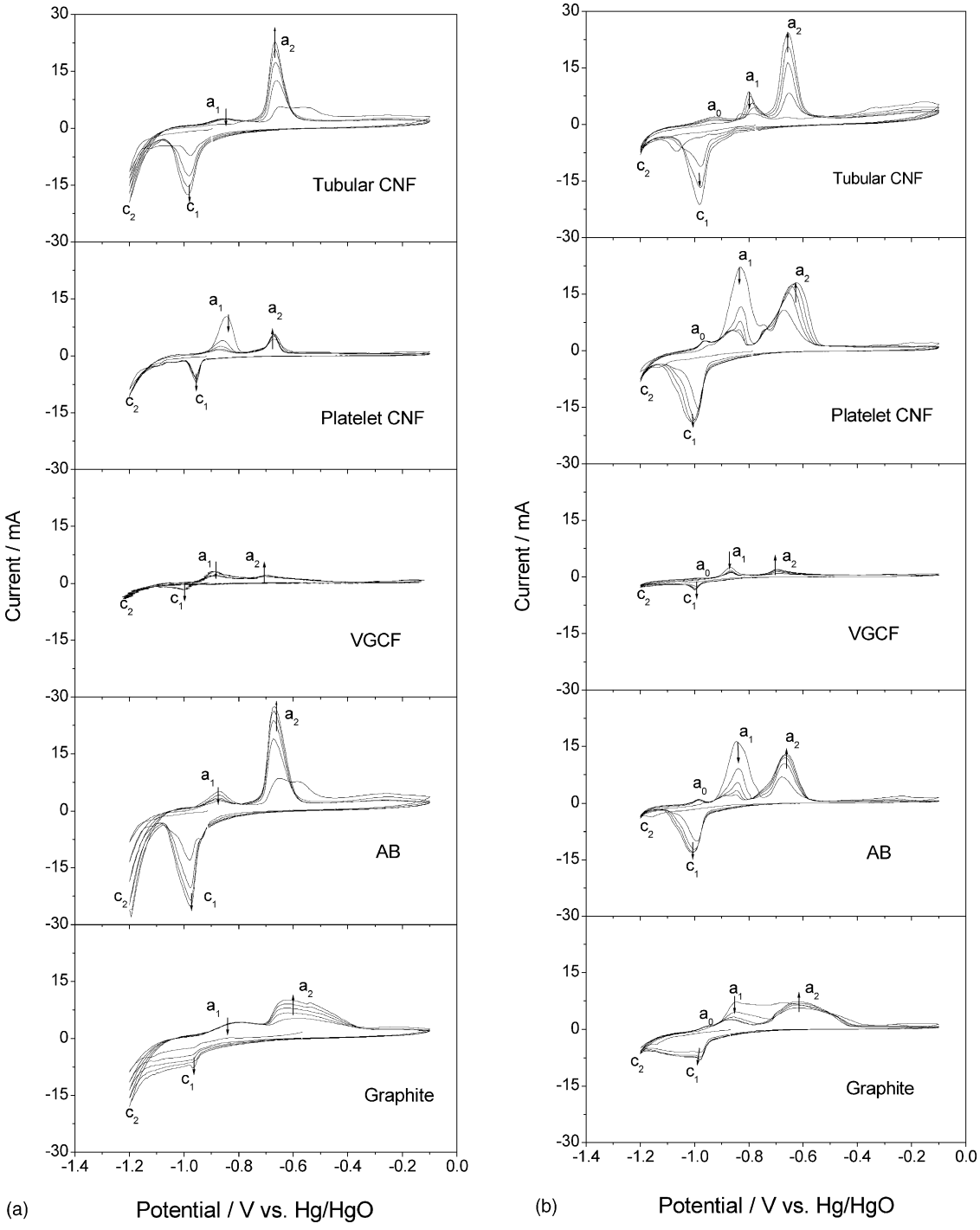

Fig. 2. Cyclic voltammetry for the Fe/C composite electrodes with Fe:C:PTFE = 45:45:10 wt.% in base electrolyte (a) and electrolyte containing 0.1 M of K_2S additive (b) after five initial cycles. (The arrows indicate the tendency of the current during the cycling.)

reduction of both Fe(III)/Fe(II) and Fe(II)/Fe. In the case of VGCF and natural graphite composite, the applied peaks were rather small and the reduction peak (c_1) was not separated sufficiently from the hydrogen evolution peak. With repetitive cycling, the redox current Fe/Fe(II) + Fe(II)/Fe(III) under (a_2) and (c_1) peak couple was increased while the current Fe/Fe(II) under peak (a_1) was decreased. This behavior is acceptable from the viewpoint that nano-carbons have a larger surface area than VGCF and graphite and then a formed $Fe(OH)_2$ layer via intermediate soluble species, $HFeO_2^-$, on nano-carbon surface should be thinner than that on VGCF and graphite. This $Fe(OH)_2$ layer is easily oxidized to Fe(III) on a nano-carbon surface, while only the thin area of $Fe(OH)_2$ was oxidized to Fe(III) on VGCF and graphite and thus a passive layer was formed. Such a thin layer distribution of Fe(III) on the nano-carbon surface resulted in a low resistance

of the electrode pellet. The redistribution of Fe species on a nano-carbon surface throughout electrochemical dissolution/deposition process of Fe was revealed in our previous study [32], leads to a large active surface area.

When K_2S was added to electrolyte (Fig. 2b), for all kind of carbons, along with the appearance of three peaks a_1, a_2 and c_1, a new anodic peak a_0 was occurred around −0.95 V on the forward scan.

Related to oxidation peak (a_0), previous investigations showed that it has been attributed either to the oxidation of adsorbed hydrogen on the electrode surface [25] or to oxidation of iron, probably to $Fe(OH)_2$ [24,28] or to soluble species $HFeO_2^-$ [19], or both, whereas some authors did not observe this peak on their curves. It is likely that both current peaks a_0 and a_1 involve the electrooxidation of iron to Fe(II) species. Cerny et al. [14] summarized the results of numerous literatures and concluded that the first step (a_0) in the oxidation of iron appears more probably than oxidation of hydrogen. This step should be formulated as $Fe \rightarrow [Fe(OH)]_{ads}$ (Eq. (2)) contrasting with $Fe \rightarrow Fe(OH)_2$ (Eq. (1)) proceeding in peak (a_1) [14]. In our case, peak (a_0) appears only with addition S^{2-} ion. Consequently, it is more probable that peak (a_0) is due to oxidation of iron to $[Fe(OH)]_{ads}$. Hence, due to the presence of K_2S additive, the reaction rate for Fe/Fe(I) increased. Thus, in this case, the appearance of peak a_1 is due to the oxidation of Fe(I) to Fe(II) as a result of reaction (3) or (4) and (5).

Comparison with Fe/C electrode in based electrolyte (Fig. 2a), in the presence of K_2S (Fig. 2b), the oxidation of $Fe(OH)_{ad}$ to $Fe(OH)_2$ (Eqs. (3) or (4), (5)) at around −0.85 V (a_1) was improved along with the occurrence of a peak for the oxidation of iron to an intermediate species around −0.95 V (a_0) (Eq. (2)). This suggests that the reaction rate of Eq. (2) was increased by sulfide ion. This result is in agreement with those in earlier literatures [5,9,10,12,14,16,21,23]. On the other hand, the redox current of both Fe/Fe(II) and Fe(II)/Fe(III) couples under peaks (a_2) and (c_1) (Eqs. (1), (6) and (7)) was also improved as indicated by their larger current compared to the absence of sulfide ion when tubular CNF and platelet CNF was employed. Further cycling reduces the current Fe(I)/Fe(II) under peak (a_1) while the redox current of Fe/Fe(II) + Fe(II)/Fe(III) couple (a_2 and c_1) was increased. This suggests that the surface area of iron active material increased with cycling.

In order to observe clearly the effect of K_2S additive on electrochemical behavior of Fe/C electrode, the capacity of oxidation reaction of Fe/Fe(II) ($a_0 + a_1$) and both Fe/Fe(II) and Fe(II)/Fe(III) (a_2) as well as discharge capacity of Fe/C electrode ($a_0 + a_1 + a_2$) at the 5th cycle was calculated from Fig. 2 and presented in Figs. 3 and 4. It is clear that the presence of K_2S in electrolyte favoured the dissolution of iron to Fe(II) and Fe(II) to Fe(III) as evidenced by increase in capacity of Fe/Fe(II) and Fe/Fe(II) + Fe(II)/Fe(III) reactions as well as discharge capacity of Fe/C electrode. However, this effect depends on the carbon and concentration of K_2S. For example, capacity of Fe/Fe(II) oxidation reaction was increased with almost all the carbons while capacity of

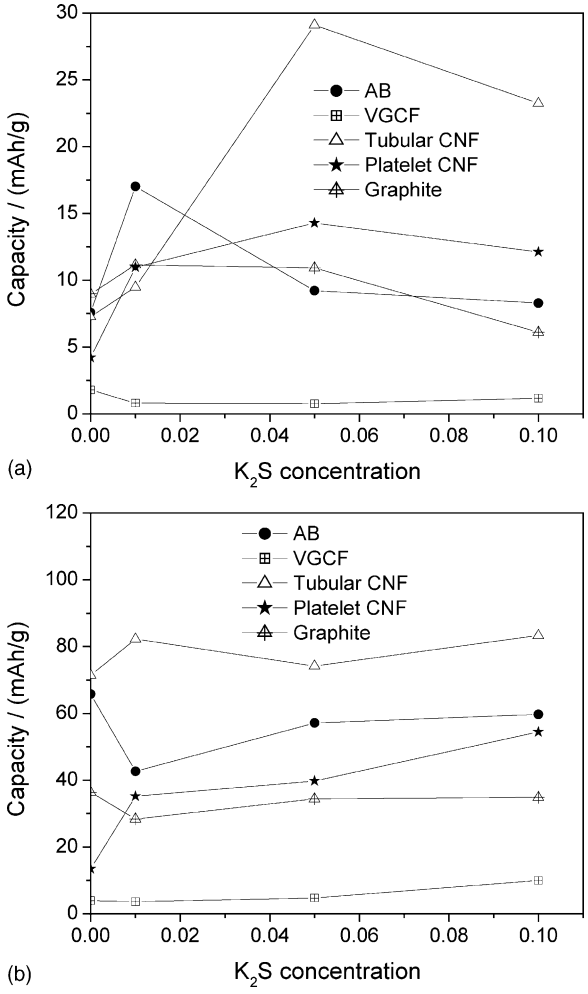

Fig. 3. The dependence of the capacity of the Fe/Fe(II) (a) and Fe/Fe(II) + Fe(II)/Fe(III) (b) oxidation reactions on K_2S concentration for Fe/C electrodes in additive-containing electrolyte.

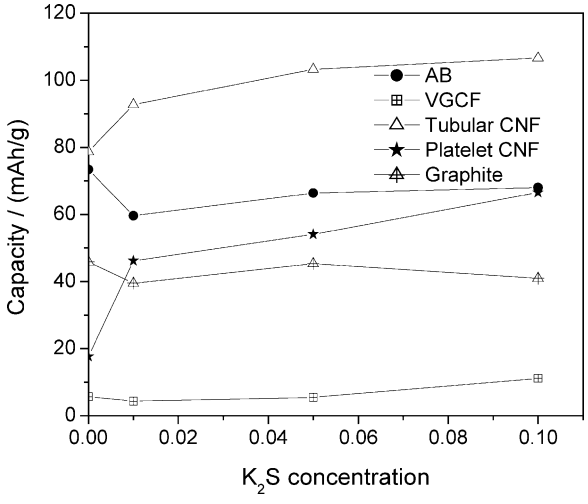

Fig. 4. Dependence of the discharge capacity of the Fe/C electrode on K_2S concentration in additive-containing electrolyte.

Fe/Fe(II) + Fe(II)/Fe(III) reaction only improved for tubular CNF, VGCF and particularly platelet CNF (Fig. 3). However, the discharge for Fe/tubular CNF and Fe/platelet CNF electrodes increased to a greater extent than that for Fe/VGCF. Therefore, the carbon morphology shows an effect on the redox behavior of the Fe/C electrode in the presence of the additive. As mentioned above, $Fe(OH)_2$ was more highly distributed on the nano-carbon surface than on VGCF and graphite during the charge/discharge via soluble intermediate species, $HFeO_2^-$. This $Fe(OH)_2$ layer is easily oxidized to Fe(III) on a nano-carbon surface, while only the thin area of $Fe(OH)_2$ was oxidized to Fe(III) on VGCF and graphite. Additionally, in the presence of S^{2-} ion in electrolyte, it may be due to the adsorbed sulphide ion interacts strongly with Fe(I) or Fe(II) or Fe(III) in the oxide film and makes breakdown of the oxide film [8,12] leading to the substantial iron dissolution and supports for the formation of $Fe(OH)_2$ on carbon surface via intermediate soluble species, $HFeO_2^-$. Further, the presence of S^{2-} increases the bulk electrical conductivity of electrode [10,15,22,23] leading to the dissolution of $Fe(OH)_2$ or the underlying metal by the ion transport through the oxide layer can be take placed. The oxidation of $Fe(OH)_2$ formed on carbon surface to Fe(III) depends on the carbon. When nano-carbons, that have large surface area, were employed, $Fe(OH)_2$ film is easily oxidized to Fe(III) than other carbons resulting in the increase in capacity of Fe(II)/Fe(III) reactions for Fe/nano-carbon electrode. On subsequent sweeping, passivation of $Fe(OH)_2$ film is formed leading to the decrease in capacity of Fe/Fe(II) reaction.

From Fig. 4, it can be seen that, the presence of K_2S benefited the Fe/C electrode when using nano-carbon such as tubular CNF, platelet CNF and VGCF. The capacities of these electrodes were increased compared with that of correspondence electrodes in based electrolyte. The largest capacities of these electrodes attained at 0.1 M K_2S. It may be due to the adsorption of S^{2-} ion on Fe/C electrode, based on the different surface area and structure of carbons, was favoured by nano-carbon with fiber structure such as tubular CNF, platelet CNF and VGCF. When the carbon component was AB or graphite, the oxidation of iron was not improved by the K_2S additive, as evidenced by the poor capacity compared with the sulfide-free case.

On the other hand, from Fig. 2, it is clear that the hydrogen evolution was suppressed significantly by K_2S for all the carbons. Two paths for the hydrogen electrode evolution in alkaline solution were supposed [9]:

$$\text{A primary step}: H_2O + e^- \rightarrow H_{ad} + OH^- \quad \text{(I)}$$

coupled either with the electrochemical desorption step

$$H_2O + H_{ad} + e^- \rightarrow H_2 + OH^- \quad \text{(II)}$$

or with the molecular recombination desorption step

$$H_{ad} + H_{ad} \rightarrow H_2 \quad \text{(III)}$$

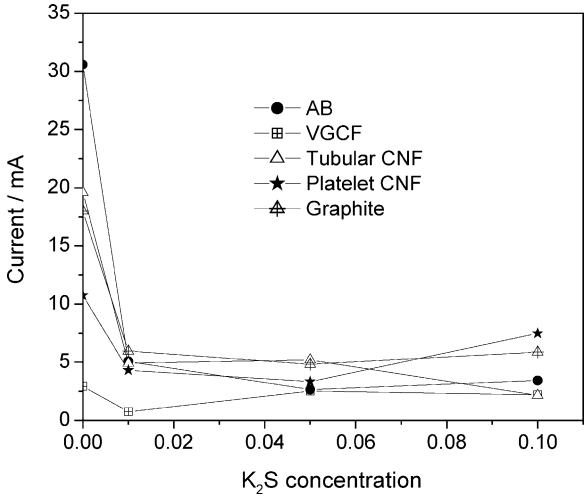

Fig. 5. Variation of the hydrogen evolution current of Fe/C electrodes on K_2S concentration in additive-containing electrolyte at −1.2 V.

Fig. 5 presents the variation of current, which was attributed to hydrogen evolution at −1.2 V, with the concentration of the K_2S additive. Compared with the Fe/C electrodes in electrolyte free of K_2S, hydrogen evolution was much decreased, especially at 0.05 M K_2S for all carbons. This result is in agreement with those results reported earlier [6–8,17] and the main reason is due to the absorption of the highly polarization S^{2-} ion. Carta et al. [9] claimed that the molecular recombination reaction (step III) was inhibited by S^{2-} ion chemisorption. Another possible reason is the change of surface species probably also influences the overpotential of the hydrogen evolution reaction [24].

3.2. Effect of FeS additive to electrode

The voltammogram of the Fe/C electrode without and with 1 wt.% FeS additive in based electrolyte at five initial cycles was presented in Fig. 6. It can be seen that, similar to K_2S additive, FeS additive and the carbon component also strongly affect on the redox behavior of iron. For the Fe/C electrode containing 1 wt.% of FeS (Fig. 6b), the forward scan revealed two oxidation peaks of Fe(I)/Fe(II) (Eqs. (3) or (4) (5)) and both Fe/Fe(II) (Eq. (1)) +Fe(II)/Fe(III) (at the first scan Eqs. (6) and/or (7), from the second scan, Eq. (7)) occurring around −0.85 V (a_1) and −0.65 V (a_2), respectively, and a small oxidation peak to form $Fe(OH)_{ad}$ species around −0.95 V (a_0) (Eq. (2)). A single reduction peak of both Fe(III)/Fe(II) and Fe(II)/Fe was occurred around −1.0 V (c_1) on the reverse scan. Similar with K_2S additive, for the all carbon used, the reduction peak of iron deposition was supported by FeS and was separated from hydrogen evolution peak around −1.2 V (c_2). Addition of FeS to electrode supported to the dissolution of Fe to Fe(II) and both Fe to Fe(II) and Fe(II) to Fe(III) at around −0.85 V (a1) and −0.65 V (a_2), respectively, along with occurrence of the intermediate species around −0.97 V (a_0). The dependence of capacity of Fe/Fe(II) ($a_0 + a_1$)

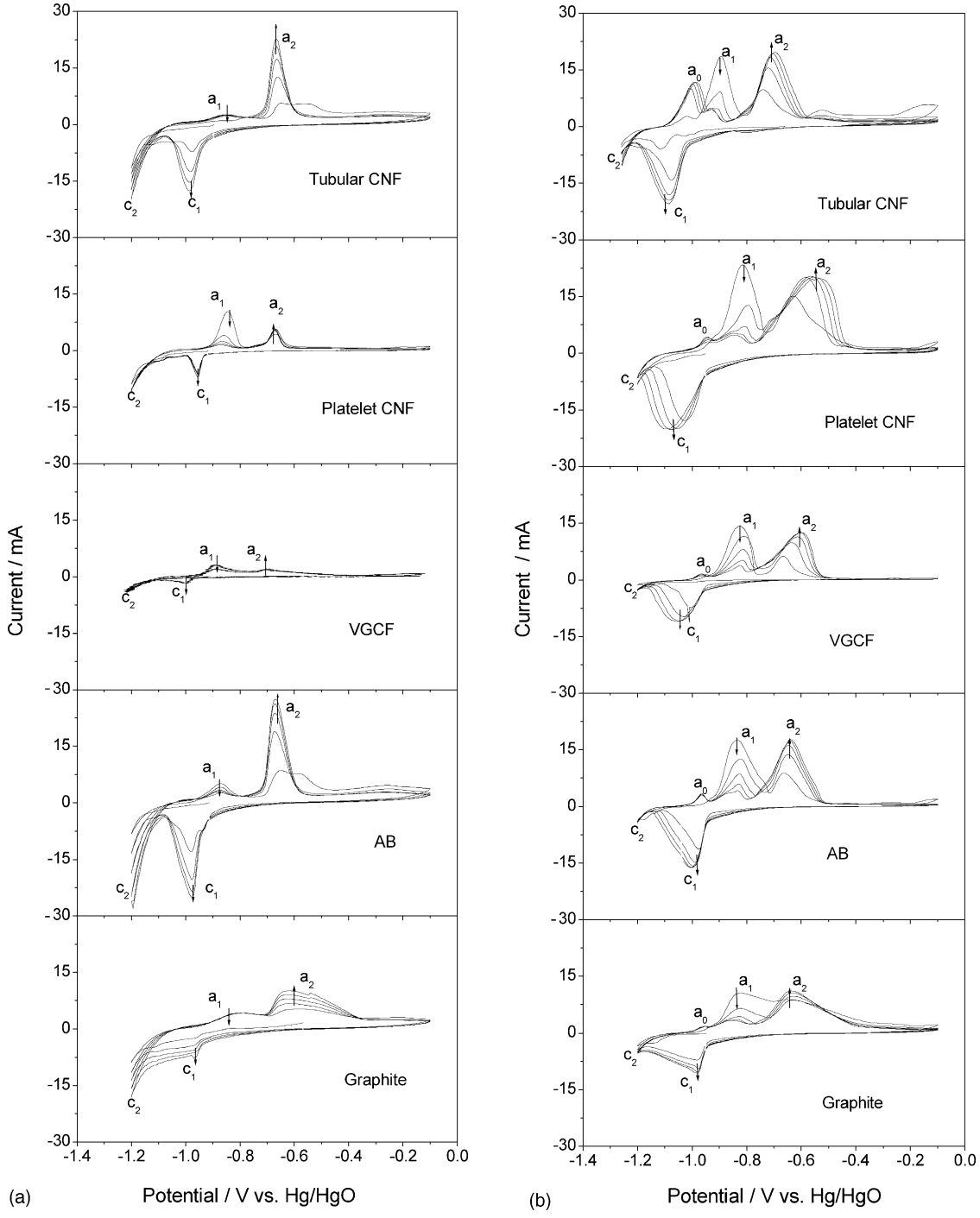

Fig. 6. Cyclic voltammetry for Fe/C composite electrodes with Fe:C:PTFE = 45:45:10 wt.% without (a) and with FeS additive (b) after five initial cycles. (The arrows indicate the tendency of the current during the cycling.)

and Fe/Fe(II) + Fe(II)/Fe(III) (a_2) oxidation reactions and discharge capacity of Fe/C electrode ($a_0 + a_1 + a_2$) on FeS content in Figs. 7 and 8 revealed that the oxidation of iron was more improved compared with Fe/C free FeS additive as well as Fe/C electrode in electrolyte containing K_2S. However, the oxidation of Fe/Fe(II) + Fe(II)/Fe(III) (a_2) was more supported by the presence of FeS than Fe/Fe(II) (a_1) and depends on the carbon and content of FeS. For example, in the case of Fe/AB, K_2S additive showed the negative effect on the discharge capacity but for FeS additive its discharge capacity was improved with the addition of 2 wt.% FeS. For the Fe/VGCF electrode, its capacity was increased significantly with FeS additive and much larger than that of K_2S additive. The capacity of Fe/graphite electrode was not improved with both FeS and K_2S additives. From these results, it confirmed that, beside the FeS additive effects, morphology of carbon

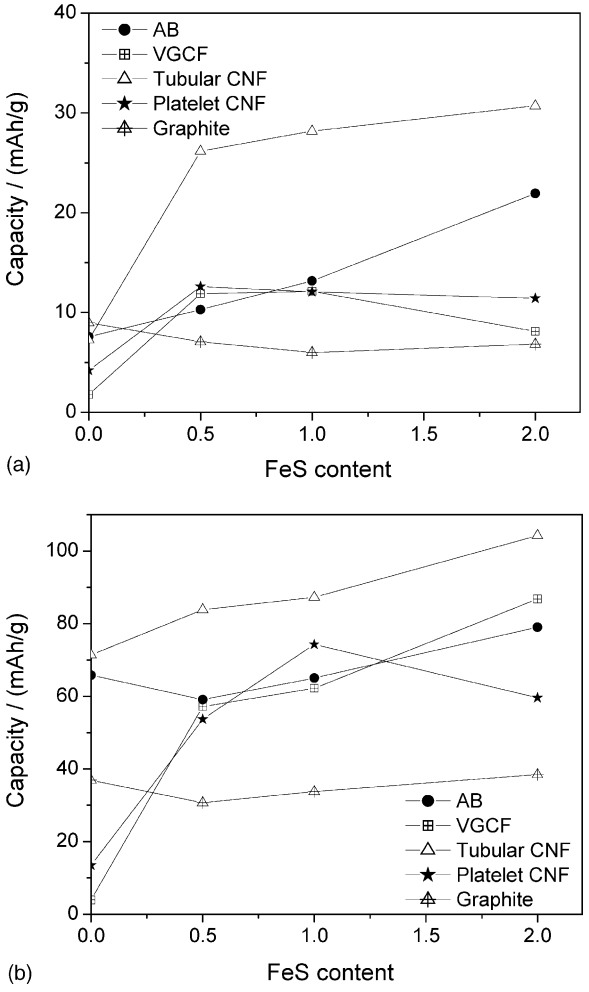

Fig. 7. Dependence of the capacity of the Fe/Fe(II) (a) and Fe/Fe(II) + Fe(II)/Fe(III) (b) oxidation reactions on FeS content for Fe/C electrodes with FeS additive.

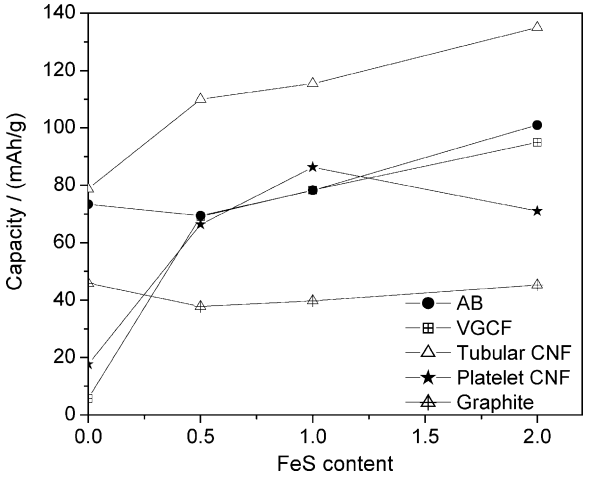

Fig. 8. Dependence of the discharge capacity of Fe/C electrodes with FeS additive on FeS content.

strongly affected on the redox behaviors of Fe/C electrode. Thus, addition of ferrous sulfide to Fe/C electrode improved its cycleability when tubular CNF, platelet CNF, VGCF and AB were employed (Fig. 8). The largest capacities for tubular CNF, VGCF and AB were attained at 2 wt.% FeS, while the largest capacity for platelet CNF was obtained at 1 wt.% FeS.

On subsequent sweeping, anodic peaks were moved to more positive potential and cathodic peak to more negative potential leading to increase in the overpotential of Fe/Fe(II) and Fe(II)/Fe(III) couple. Similar with K_2S additive, with repeating cycling reduces the current under Fe(I)/Fe(II) peak (a_1) while the redox current of Fe/Fe(II) + Fe(II)/Fe(III) (a_2) couple was increased. This suggests that the thickening of the oxide film took place with subsequent cycling. The formation of Fe(II) was inhibited with subsequently cycle but the formation of Fe(III) was favoured. This result indicated the surface area of iron active material was increased with cycling. On the other hand, passivation of $Fe(OH)_2$ film is formed leading to the decrease in capacity of Fe/Fe(II) reaction. The explanation for this behavior is similar with K_2S additive. The main reason may be due to the adsorbed sulphide ion, which interacts strongly with Fe(I) or Fe(II) or Fe(III) in the oxide film and makes breakdown of the oxide film [8,12] leading to the substantial iron dissolution and supports for the formation of Fe(II) and Fe(III). In addition, carbons used also strongly affect on the distribution of $Fe(OH)_2$ on their surface. As above description, nano-carbons have larger surface area than VGCF and graphite, thereby, $Fe(OH)_2$ film formed on nano-carbons via intermediate soluble species, $HFeO_2^-$, should be thinner than on VGCF and graphite. This $Fe(OH)_2$ layer is easier oxidized to Fe(III) on nano-carbons than on VGCF and graphite. However, with the FeS additive, the capacities of almost all of the electrodes were improved and were larger than those with the K_2S additive, especially for the Fe/VGCF electrode. Furthermore, capacity of Fe/AB was also improved with 2 wt.% of FeS. This may be due to the incorporation of FeS in electrode favours the adsorbed capability of S^{2-} on electrode surface results in breaking easier of oxide layer.

Another possibility may be due to the adsorbed sulfide ion also causes a distortion in $Fe(OH)_2$ structure leading to an increase in defect concentration of the film and consequently its ionic conductivity rises. Obviously, this retards the passivation process [22] and thicker film formed.

Comparison the effect of FeS and K_2S additive on capacity of Fe/C electrode indicates that with FeS additive, for almost carbons, the capacities of Fe/C electrodes were more increased than K_2S additive (Figs. 4 and 8). This behavior may be explained based on the basic of the dissolution of FeS to form Fe^{2+} and S^{2-}. The iron content of Fe/C electrode with FeS additive was increased resulting in the higher capacity of electrode contained FeS than that of electrode in K_2S additive. Additionally, under the experimental conditions of the present study, the concentration of S^{2-} in the presence of the FeS additive may be higher than that with the K_2S additive, thereby further enhancing the dissolution of iron.

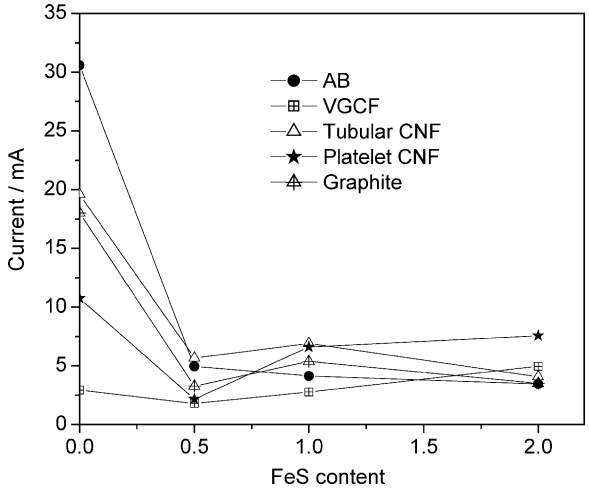

Fig. 9. Variation of hydrogen evolution current of Fe/C electrodes with FeS additive on FeS concentration at −1.2 V.

Similar to K_2S, hydrogen evolution was suppressed significantly by FeS additive for all Fe/C electrodes as presented in Fig. 9. Compared with electrode Fe/C free FeS, hydrogen evolution was much decreased, especially at 0.5% FeS for all carbons. The reduction of hydrogen evolution supports for charge efficiency and discharge capacity for Fe/C electrode.

Comparison of the effect of K_2S and FeS on the behavior of Fe/C electrode suggests that FeS showed the more benefit than K_2S additive.

4. Conclusion

The roles of the K_2S and FeS additives in determining the behavior of the Fe/C electrode were interpreted based on the presence of adsorbed sulphide ion. Ion sulphide interacts with Fe(I), Fe(II) and Fe(III) in the oxide film to promote the dissolution of iron and enhance the bulk conductivity of the electrode, leading to improvements in the cycleability.

Hydrogen evolution was suppressed significantly by using both FeS and K_2S additives.

Discharge capacity of Fe/C was improved with both FeS and K_2S when using tubular CNF, platelet CNF and VGCF. Discharge capacity of Fe/AB electrode was only favoured when using FeS additive at 2 wt.%. Both these additives showed the negative effect with natural graphite.

Acknowledgement

This work was supported by the CREST program of JST (Japan Science and Technology Agency).

References

[1] C. Chakkaravarthy, P. Perasamy, S. Jegannathan, K.I. Vasu, J. Power Sources 35 (1991) 21–35.
[2] K. Vijayamohanan, T.S. Balasubramanian, A.K. Shukla, J. Power Sources 34 (1991) 269–285.
[3] M. Jayalakshmi, B.N. Begumi, V.R. Chidambaram, R. Sabapathi, V.S. Muralidharan, J. Power Sources 39 (1992) 113–119.
[4] N. Jayalakshimi, V.S. Muralidharan, J. Power Sources 56 (1995) 209–212.
[5] N.A. Hampson, R.J. Latham, A. Marshall, R.D. Giles, Electrochim. Acta 19 (1974) 397–401.
[6] L. Ojefors, Electrochim. Acta 21 (1974) 263–266.
[7] P.R. Vassie, A.C.C. Tseung, Electrochim. Acta 21 (1976) 299–302.
[8] D.W. Shoesmith, P. Taylor, M.G. Bailey, B. Ikeda, Electrochim. Acta 23 (1978) 903–916.
[9] R. Carta, S. Dernini, A.M. Polcaro, P.F. Ricci, G. Tola, J. Electroanal. Chem. 257 (1988) 257–268.
[10] K. Vijayamohanan, A.K. Shukla, S. Sathyanarayana, J. Electroanal. Chem. 289 (1990) 55–68.
[11] K. Vijayamohanan, A.K. Shukla, S. Sathyanarayana, J. Electroanal. Chem. 295 (1990) 59–70.
[12] G.P. Kalaignan, V.S. Muralidharan, K.I. Vasu, J. Appl. Electrochem. 17 (1987) 1083–1092.
[13] K. Micka, Z. Zabransky, J. Power Sources 19 (1987) 315–323.
[14] J. Cerny, K. Micka, J. Power Sources 25 (1989) 111–122.
[15] K. Vijayamohanan, A.K. Shukla, J. Power Sources 32 (1990) 329–339.
[16] N. Jayalakshimi, S. Muralidharan, J. Power Sources 32 (1990) 341–351.
[17] T.S. Balasubramanian, A.K. Shukla, J. Power Sources 41 (1993) 99–105.
[18] J. Cerny, J. Power Sources 45 (1993) 267–279.
[19] P. Periasamy, B.R. Babu, S.V. Iyer, J. Power Sources 58 (1996) 35–40.
[20] P. Periasamy, B.R. Babu, S.V. Iyer, J. Power Sources 62 (1996) 9–14.
[21] P. Periasamy, B.R. Babu, S.V. Iyer, J. Power Sources 63 (1996) 79–85.
[22] C.A. Caldas, M.C. Lopes, I.A. Carlos, J. Power Sources 74 (1998) 108–112.
[23] C.A.C. Souza, I.A. Carlos, M.C. Lopes, G.A. Finazzi, M.R.H. de Almeida, J. Power Sources 132 (2004) 288–290.
[24] R.S. Schrebler-Guzman, J.R. Viche, A.J. Arvia, Electrochim. Acta 24 (1979) 395–403.
[25] V.S. Muralidharan, M. Veerashanmugamani, J. Appl. Electrochem. 15 (1985) 675–683.
[26] O. Khaselev, J.M. Sykes, Electrochim. Acta 42 (1997) 2333–2337.
[27] R.D. Armstrong, I. Baurhoo, J. Electroanal. Chem. 40 (1972) 325–338.
[28] D.D. Macdonald, D. Owen, 120 (1973) 317–324.
[29] L. Ojefors, J. Electrochem. Soc. 123 (1976) 824–828.
[30] L. Ojefors, J. Electrochem. Soc. 123 (1976) 1691–1696.
[31] L. Ojefors, J. Electrochem. Soc. 123 (1976) 1139–1144.
[32] T.H. Bui, M. Egashira, I. Watanabe, S. Okada, J. Yamaki, S. Yoon, I. Mochida, J. Power Sources 143 (2005) 256–264.